Supplemental material for: Kondo screening and random-singlet formation in highly disordered systems

Lucas G. Rabelo,[1] Igor C. Almeida,[2] Eduardo Miranda,[3] Vladimir Dobrosavljević,[4] and Eric C. Andrade[1]

[1] *Instituto de Física, Universidade de São Paulo, 05315-970, São Paulo, SP, Brazil*
[2] *Instituto de Física de São Carlos, Universidade de São Paulo, São Carlos, SP, 13560-970, Brazil*
[3] *Gleb Wataghin Physics Institute, The University of Campinas, Rua Sérgio Buarque de Holanda, 777, CEP 13083-859 Campinas, SP, Brazil*
[4] *Department of Physics and National High Magnetic Field Laboratory, Florida State University, Tallahassee, FL 32306*

(Dated: September 30, 2026)

S1. FURTHER DETAILS OF THE MODEL AND OF THE LARGE–$\mathcal{N}$ SOLUTION

We present further details of the mean-field solution of the two-impurity Kondo problem.

A. Clean case

To illustrate the physical content of our solution to the two-impurity Kondo problem, we study two magnetic impurities interacting with a clean (homogeneous) conduction electron bath. For simplicity, we work on a square lattice with nearest-neighbor hopping t and assume local Kondo couplings, $K^a_{ij} = J^a_K \delta_{iA}\delta_{jA}$ and $K^b_{ij} = J^b_K \delta_{iB}\delta_{jB}$, where $J^a_K = 8t^2_{aA}/U$ and $J^b_K = 8t^2_{bB}/U$. The local assumption implies that impurity a (b) couples only to the lattice site $|A\rangle$ ($|B\rangle$) located at $\boldsymbol{r}_A$ ($\boldsymbol{r}_B$). Importantly, in the single-impurity regime — where a single local moment d couples locally to the origin site $|o\rangle$ and $|\Delta| = 0$ — Eq. A4 of the main text reduces to the well-known Nagaoka–Suhl one-loop equation [1]

$$\sum_\nu \frac{|\langle o|\nu\rangle|^2}{E_\nu} \tanh\left(\frac{E_\nu}{2T^0_{K,d}}\right) = \frac{2}{J_K}, \tag{S1}$$

where $T^0_{K,d}$ is the single-impurity Kondo temperature for the local moment d.

We begin by analyzing the two-impurity Kondo problem in the uniform case $J^a_K = J^b_K = J_K$. Fig. S1(a) shows the resulting phase diagram at a fixed local Kondo coupling $J_K/t = 1$ and impurity separation $\Delta r = |\boldsymbol{r}_A - \boldsymbol{r}_B| = a_0$, where a_0 is the lattice spacing for the periodic lattice discussed in this example. For $J_{ab} = 0$, we get a finite Kondo temperature $T^{\rm pair}_K = T^0_K$ and $|\Delta| = 0$. This is the single-impurity solution, where both impurities are individually quenched by the conduction electrons below the same Kondo temperature T^0_K. As a function of J_{ab}, the Kondo temperature remains unaltered until $J_{ab} = 4T^0_K \equiv J^*_{ab}$. Beyond this point, we find a narrow window, $J_{ab} \in [J^*_{ab}, J^C_{ab}]$, where both $T^{\rm pair}_K$ and $|\Delta|$ are non-vanishing. Above a critical value J^C_{ab}, the system enters the non-Kondo (random-singlet) state with $|\Delta| = J_{ab}/2$ and $T^{\rm pair}_K = 0$. In general, this transition is discontinuous. In the coexistence region, there is a competition between Kondo screening (scale $T^{\rm pair}_K$) and random-singlet formation (scale $|\Delta|$), and we observe a slight initial increase in T_K. This occurs because the Kondo resonance at the Fermi level (for $\Delta = 0$) splits into two peaks centered at $\pm\Delta$. The Kondo temperature, defined as the half-width at half-maximum, thus increases. As we tune up J_{ab}, the DOS at the Fermi level is suppressed, and the Kondo effect disappears [2]. We also note that the coexistence region is drastically suppressed as a function of impurity separation [see inset of Fig. S1(a)].

We now investigate the clean case with different local Kondo couplings, $J^a_K \neq J^b_K$, and fix $J^a_K \geq J^b_K$ (hence $T^0_{K,a} \geq T^0_{K,b}$). As shown in Fig. S1(b), for $J_{ab} \leq 4T^0_{K,a}$, we obtain the single-impurity solution. In this case, $|\Delta| = 0$ and both moments are Kondo quenched independently, each below its own single-impurity Kondo temperature. For $J_{ab} > 4T^0_{K,a}$, we observe the emergence of a narrow coexistence region where $\Delta \neq 0$ and $T^{\rm pair}_K > 0$. The larger single-impurity Kondo temperature sets the scale in this region, whose width shrinks rapidly as the asymmetry $|J^a_K - J^b_K|$ increases.

Taken together, these results show that the two-impurity phase diagram is dominated by (i) a single-impurity regime with $\Delta = 0$, where the local moments a and b are individually quenched by the conduction electrons below $T^0_{K,a}$ and $T^0_{K,b}$, respectively, and (ii) a random-singlet regime, in which the local moments pair into a random-singlet state characterized by $|\Delta| = J_{ab}/2$ and $T^{\rm pair}_K = 0$. The coexistence solution that captures the competition between Kondo screening and random-singlet formation, where both Δ and $T^{\rm pair}_K$ are finite, occurs only within a narrow parameter window and is rapidly suppressed as the impurity separation increases and/or the Kondo temperatures become asymmetric.

B. Disordered case

To solve the problem in the disordered case, we first determine the single-impurity Kondo temperature at every dopant site. For each of the $N_{\rm imp}$ impurities, we consider an independent Kondo problem in which the chosen site acts as a local moment while the remaining $N_{\rm imp} - 1$ sites form the conduction bath. As a result, for

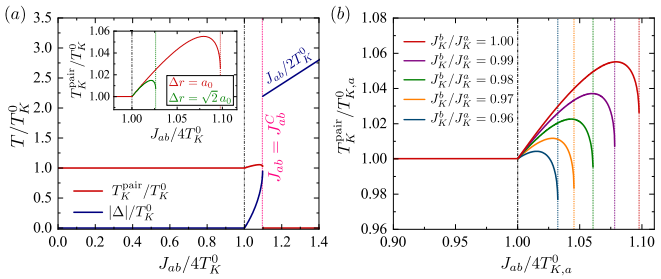


FIG. S1. Solution of the two-impurity Kondo problem in the clean limit. We model the conduction electrons as a square lattice with nearest neighbor hopping t and with $\mu = -0.1t$. (a) Phase diagram of the model with a fixed local Kondo coupling, $J_K/t = 1$, as a function of the Heisenberg exchange J_{ab}, considering impurity a (b) connected locally to the lattice site at $\boldsymbol{r}_A$ ($\boldsymbol{r}_B$), with $\Delta r = |\boldsymbol{r}_A - \boldsymbol{r}_B| = a_0$. Here, $T_K^0 = 2.88 \times 10^{-2}\, t$. Inset: Kondo temperature $T_K^{\rm pair}$ as a function of $J_{ab}/4T_K^0$ for two distinct values of Δr. (b) Kondo temperature of the model with distinct local Kondo couplings, $J_K^a \neq J_K^b$, and $\Delta r = a_0$, showing the rapid suppression of the coexistence region with increasing asymmetry $|J_K^a - J_K^b|$. Here, dotted lines indicate the critical Heisenberg coupling where $T_K^{\rm pair}$ abruptly drops to zero. The dashed-dotted line marks the condition $J_{ab} = 4T_{K,a}^0$, where $T_{K,a}^0 = 2.88 \times 10^{-2}\, t$ is the Kondo temperature calculated at $J_{ab} = 0$.

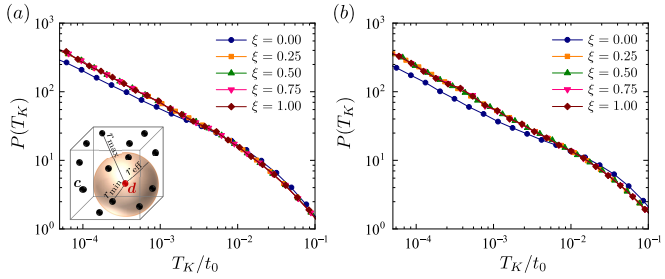


FIG. S2. Convergence of the distribution of single-impurity Kondo temperatures $P(T_K)$ as a function of the effective radius $r_{\rm eff}$ around the local moment, with $r_{\rm eff} = r_{\rm min} + \xi(r_{\rm max} - r_{\rm min})$, where $r_{\rm min}$ and $r_{\rm max}$ represent, respectively, the closest and farthest distances between the local moment and a conduction electron site. Here $L = 30$, and (a) $n = 0.010$ and (b) $n = 0.020$. Inset: pictorial representation of $r_{\rm eff}$.

every impurity choice, we generate a distinct conduction band Hamiltonian $\mathcal{H}_0$. Because our simulations employ $N_{\rm imp} \gg 1$, the spectra of $\mathcal{H}_0$ with $N_{\rm imp} - 1$ or $N_{\rm imp} - 2$ sites are virtually identical, ensuring that the single- and two-impurity calculations can be compared on an equal footing.

Importantly, for each single-impurity Kondo problem, we connect the corresponding local moment to all sites in the electronic bath. Because the hopping t_{ij} decay exponentially with the distance, we expect that the contributions from conduction sites far away from the impurities are negligible, meaning that only a subset of conduction band sites (within an effective radius $r_{\rm eff}$) significantly interact with the local moment. To speed up our calculations, we implement the following scheme. Let $r_{\rm min}$ and $r_{\rm max}$ represent, respectively, the closest and farthest distances between the local moment and a conduction electron site. We define the effective radius as $r_{\rm eff} = r_{\rm min} + \xi(r_{\rm max} - r_{\rm min})$. By this definition, $\xi = 0$ corresponds to a local coupling, whereas $\xi = 1$ corresponds to the local moments interacting with all conduction sites. We find that $\xi = 0.25$ already captures the relevant low-energy physics [see Fig. S2(a-b)], and we therefore set $\xi = 0.25$ in all the results presented in this work.

S2. LOCAL MOMENT SUSCEPTIBILITY

In the limit $n \to 0$, where we decouple the local moments from the conduction electrons, it is possible to obtain an analytical expression for the local moment susceptibility. In the original Bhatt-Lee solution, all local moments within the system interact with one another. As one removes the strongly coupled singlet, all remaining couplings are renormalized [3]. These renormalized couplings are generically smaller in magnitude with respect to the original ones, implying they affect the properties of the systems at much lower energy scales, where $Q(J_{ab})$ is already singular. Moreover, the renormalization of the remaining couplings is an effect of order $1/\mathcal{N}$ for SU($\mathcal{N}$) spins [4], making the geometrical decimation consistent with our large$-\mathcal{N}$ solution of the problem.

Using the geometrical procedure, we numerically calculate the spin susceptibility and write $\chi(T) = n_{\rm free}(T)/T$. We observe that $\chi(T)$ inherits the singularity of $Q(J_{ab})$ at low$-T$, with the singularity being more pronounced for small impurity density. To model the numerical data, one assumes that each spin defines a sphere of volume $v \propto \ell^3$, where $\ell \sim n^{-1/3}$ is the typical inter-spin distance. Since all these spheres touch each other, they are on the verge of forming a singlet but are still free. Therefore, if one relates the length scale ℓ with energy via $J_{ab} \sim \exp(-2r_{ab}/a)$, we can write $\chi(T) \sim 1/T \ln^3(t_0/T)$ [5], which is a logarithmic correction to the free moment result. Although this simple formula accurately describes the numerical data [5], we refrain from implementing it here, as the effective description of the susceptibility singularity as a power law captures the data well over the full range of n we study.

We use two complementary methods to extract the power-law exponent α. First, we extract the exponent fitting the slope of the linear behavior of $P(T_K)$ on a log-log scale. Complementarily, we extract α directly from the data [6]. We assume that $P(T_K)$ displays a power-law form in the interval $T_K < T_K^{\rm max}$, with $T_K^{\rm max}$ the upper cutoff scale below which the power-law holds. The value of $T_K^{\rm max}$ for the power-law model that

is most likely to have generated this data is given by $\alpha = 1 - \langle \ln (T_K^{\max}/T_K) \rangle^{-1}_{T_K < T_K^{\max}}$ [6]. In practice, we plot $\alpha \times T_K^{\max}$ and select the optimal $T_K^{\max}$ inside an energy window where α is reasonably stable. Both methods agree, enhancing confidence in the value of the exponent.

[1] A. C. Hewson, *The Kondo Problem to Heavy Fermions*, 1st ed. (Cambridge University Press, Cambridge, 1993).

[2] V. Dobrosavljević and G. Kotliar, Strong-coupling limit of the kondo problem, Phys. Rev. B **46**, 5366 (1992).

[3] R. N. Bhatt and P. A. Lee, Scaling studies of highly disordered spin-$\frac{1}{2}$ antiferromagnetic systems, Phys. Rev. Lett. **48**, 344 (1982).

[4] J. A. Hoyos and E. Miranda, Random antiferromagnetic SU(n) spin chains, Phys. Rev. B **70**, 180401(R) (2004).

[5] S. Zhou, J. A. Hoyos, V. Dobrosavljević, and E. Miranda, Valence-bond theory of highly disordered quantum antiferromagnets, Europhys. Lett. **87**, 27003 (2009).

[6] A. Clauset, C. R. Shalizi, and M. E. J. Newman, Power-law distributions in empirical data, SIAM Review **51**, 661 (2009).